Magazine of Civil Engineering

ISSN 2712-8172

journal homepage: http://engstroy.spbstu.ru/

DOI: 10.34910/MCE.108.8

Behavior of CFT steel columns damaged by thermal shock

R. Al-Rousan

Jordan University of Science and Technology, Irbid, Jordan

E-mail: rzalrousan@just.edu.jo

Keywords: cyclic lateral loads, fiber reinforced polymer, nonlinear, finite element analysis

Abstract. Experimental evaluation of the structural behavior of concrete-filled tubular (CFT) circular steel columns under the combined effects of axial and cyclic lateral loads is costly and challenging. Therefore, this study provides a nonlinear finite element analysis (NLFEA) of fourteen models for thermal shock damaged CFT circular steel columns wrapped with various layers of carbon fiber reinforced polymer (CFRP) composites at its end region, which represents the critical location in terms of the lateral load capacity. Firstly, the column axial load was applied as the first loading step, and then the horizontal load was applied at the top of the column as displacement-controlled loading to guarantee the descending part of the load-displacement behavior. The intent is to confine the column end to avoid outward local buckling of the CFT column and thus developing high strength, larger net drift and more energy dissipation. The NLFEA models were properly calibrated and validated with reputable experimental results, followed by conducting a parametric study to assess the influence of the number of CFRP layers and the impact of thermal shock on the CFT circular steel column performance. For the modeled CFT circular steel column, the use of five to ten layers of CFRP composites resulted in a significant performance enhancement. However, the performance enhancements using 9 and 10 CFRP layers were comparable with 8 CFRP layers. In addition, it was found that the column axial load level significantly affects the CFT circular steel column behavior under lateral loading; better behavior as the axial load level increased. Strengthening of any CFT circular steel column must be optimized through proper NLFEA modeling and the findings of this study represent useful guidelines and methodology for the similar strengthening of CFT steel columns damaged by thermal shock.

1. Introduction

In the outward direction, the local buckling has been a source of disturbance for practitioners in the field of concrete-filled tubular (CFT) steel columns. In addition, such columns are always exposed, aside from the axial load, to seismic forces and/or sideways winds, resulting in generating moments close to the columns' ends, in particular. That makes that region- the columns end- a risky one. Therefore, it is essential to design highly-ductile, resistant-to-moment columns, able to in a way that is capable of undergoing lateral, plastic deformation. Several researchers have investigated the performance of the steel CFT columns [1–2].

Overloading structures and exceeding their ultimate loads, such as heavy trafficking on a bridge or increasing the number of stories in a building, necessitates the structural elements to be reinforced and repaired. To resolve the issue of overloading, the structural elements can be either reconstructed or retrofitted, aiming to enhance the element's load capacity. However, the reconstruction process is not so preferable because it is time-consuming and costly; this process may harm the nearby elements when knocking down a structure due to the generated vibratory force. In contrast, the retrofitting process saves time and more cost-effective, particularly for real old buildings. In some countries, such as India, the design of most of the buildings does not abide by the standard seismic codes; therefore, such structures cannot withstand strong earth shakes. So, these structures need to be retrofitted to increase their seismic capacity.

Al-Rousan, R. Behavior of CFT steel columns damaged by thermal shock. Magazine of Civil Engineering. 2021. 108(8). Article No. 10808. DOI: 10.34910/MCE.108.8

There are many retrofitting columns; the steel and concrete jacketing and the fiber-reinforced polymer (FRP). The FRP has been widely adopted worldwide because high in tensile capacity, not costly, non-corrosive, and easy to shape and erect. There are many types of FRP materials available, namely: carbon fiber-reinforced polymers (CFRP), glass fiber, reinforced polymer (GFRP), and aramid fiber-reinforced polymer (AFRP). However, the FRP materials have a setback; as its mode of failure is de-bonding, the FRP-concrete bond is sudden and brittle. A number of studies related to this field were conducted to investigate the reinforced concrete (RC) columns' performance when they were subjected to loads, concentrically and eccentrically [3]. It has been found that it is urgent to strengthen the damaged and deteriorated RC columns due to the additional loads from earthquakes and other environmental situations. The techniques of steel plate jackets and the RC jackets have been broadly used in strengthening the RC columns. However, it has been observed that these techniques have several problems: they are time consumers because of the slowness of the curing; they are material consumers because they require the columns to be bigger, in addition to the material characteristics. To avoid such obstacles, a new method was introduced at the beginning of the eighties of the last decade, which was to externally confine the concrete columns with wraps of CFRP composite material. This technique has improved the strengthened columns' ductility and load capacity because the CFRP materials are: cost-effective, time-saving, easy to shape and erect, non-corrosive, and have an ultra-strength-to-weight ratio. To find a way to strengthen the CFT columns further and avoid the outward local buckling, Alrousan et al. [4] suggested to confine the ends of the columns with FRP. Furthermore, confining the ends of columns has enhanced the performance quality of the internal concrete, particularly in the ends at which high stresses develop [4–6]. The method of confining the CFT steel columns with FRP has been the focus of a number of experimental and investigatory researches [7–13]. Among those, they were investigating the behavior of circular CFT columns, confined with glass FRP, when exposed to 1) axial compression with the monotonic application [6], and 2) cyclic axial compression [14, 15]. On the other hand, very few researches have been showing to investigate the seismic behavior of FRP confined CFT steel columns [7, 8, 11]. These studies showed a remarkable enhancement in the circular-shaped and square-shaped CFT steel columns' behavior quality when confined with FRP.

It is common knowledge that the RC elements are subjected to severe harms or damages when encountering very high temperatures. RC beams, for instance, when RC beams are exposed to excessive degrees of temperatures beyond 250 °C, the concrete's and the steel's mechanical characteristics will be altered, causing stresses to be redistributed; In consequence, their stiffness and toughness are lessened, and they will suffer big deformations, permanently [16, 17]. At present, the CFRP sheets are being widely utilized to rehabilitate the heat-damaged RC beams. That is because these sheets are non-corrosive, time-saving, cost-effective, easy to shape, very applicable, and simple to install on the structural elements. Several studies stated that the heat-damaged beams could- to an extent- re-gain their flexural capacity and improve their behavior when they were bonded, from the external side, with sheets of CFRP. Nevertheless, this is governed by a number of factors, namely: the element's resistivity to fire [18], the structure's ability to withstand very high temperatures [19, 20], the type of fiber used [21–24], the type of analysis [25–29], the energy integrity resistance [30], the utilized method of anchoring [31], the conditions of heating [32, 33], the severity of the damage, the beam's geometry, and the utilized type of fiber sheet [34], in addition to the adopted safety factors when reinforcing the bridges by CFRP [35].

RC structures (e.g., near-to-furnace, chimneys, rocket launcher sites, power plants) are frequently exposed to consistent heating-cooling cycles. Such cycles endanger the structural stability and demand certain requirements upon designing [36, 37]. It is of common knowledge that concrete can withstand heat till 250-300 °C before it begins to weaken. Beyond 500 °C, the mechanical features of concrete decrease, to a great extent. In addition, another cause of concrete weakening is rabid cooling, e.g., putting out a fire attack with cool water, as this method produces a big difference in the temperature between the concrete surface and its core, causing cracking of concrete due to the development of high superficial tensile stresses. This is another form of damage of structures caused by the weakening of the aggregates' quality and the adjoining paste due to the frequent, incompatible expansions and contractions. It must be mentioned that several factors determine the severity of the damage, such as the structure's size, the sort of the utilized cement and aggregates, the amount of moisture contained in concrete, the time and the frequency the structure is exposed to heat, the cooling mechanism, and the attained maximum degree of temperature [38]. To modify and strengthen the already standing concrete structures, various methods have been utilized, for example RC jacketing, bolting steel plates, prestressed external tendons, and the newly-developed FRP materials. The FRP composites technique has been adopted in various parts of the world for its many features, namely: highly strong, ductile, resistant to corrosion, easy to shape and erect, viable in many applications, high strength-to-weight ratio; keeping in mind that the majority of concrete structures are subjected to damage because of steel corrosion, frequent cycles of freezing and thawing, and dynamic loads [39, 40].

For the past two decades, using CFRP materials to repair and strengthen the RC structures has been a focus worldwide. Many researchers studied RC structures' behavior, CFT columns in particular when externally reinforced by laminates of CFRP. It is worth noting that it is very complicated to examine CFT columns' behavior when exposed to both axial and cyclic lateral loadings. This experiment requires a high-capacity testing machine and a specially-designed setup, which are not easy to attain. The nonlinear finite analysis (NLFEA) method has been utilized to validate the obtained test results, as this method can produce close-to-real results. With adequate validation, the NLFEA method can be employed to examine the reinforced-by-external-CFRP elements impacted by many parameters, such as the thickness of the CFRP layers. What has made it urgent to conduct the study in hand is the severe shortage of information about CFT columns' behavior damaged by thermal shock, which hinders further expansions in this field. In this study, the NLFEA program was used to investigate the influence of externally confining the heat-damaged CST columns, with CFRP materials, on the columns ductility and strength, aiming to obtain out-of-the-box results.

Testing CFT columns under combined axial and cyclic lateral loading is a challenge since it requires a special setup and testing machine with unique capacities. The availability of sound experimental test results is considered priceless and can be used to create and validate robust NLFEA simulating the actual ones. Therefore, this study presents an advanced NLFEA model for predicting seismic behavior and mode of failure of CFRP-confined CFT circular steel columns. To simulate the real behavior of CFT circular steel columns, experimentally obtained relationships for the mechanical characteristic of concrete were incorporated in the simulating process [41], along with suitable models for the various components of the CFT circular steel columns, including concrete, steel tube, and testing conditions. The first step, in this paper, includes the validation of the CFT circular steel model against the published experimental results by Yu et al. [41] and then was expanded to consider the effect of the number of CFRP layers (zero (control), five, six, seven, eight, nine and ten layers) subjected to room temperature (un-damaged) and thermal shock (damaged). The theoretically generated data included stress contours, horizontal load-displacement hysteretic loops, lateral load, net drift capacities, horizontal displacement-steel strain responses, horizontal displacement-CFRP strain responses, stiffness degradation, performance enhancement factor, and energy dissipation. In all simulations, realistic constitutive laws for materials, reasonable interface models, and the reliable verified factors were adopted.

2. Methods

2.1. Experimental Work Review

Fig. 1 shows the specimen's geometric details and a schematic diagram of the experimental test set-up [41]. The CFT column is 318 mm in diameter and 1625 mm in the height of 1625 mm connected rigidly to a stiff, reinforced concrete footing that is 1500 mm long, 1400 mm wide, and 550 mm thick. The steel tube used in all specimens is 3 mm thick with a diameter to thickness ratio of 106. The confinement at the column end (500 mm) was provided using a CFRP jacket to allow full plastic hinge formation and developing a high toughness and ductility.

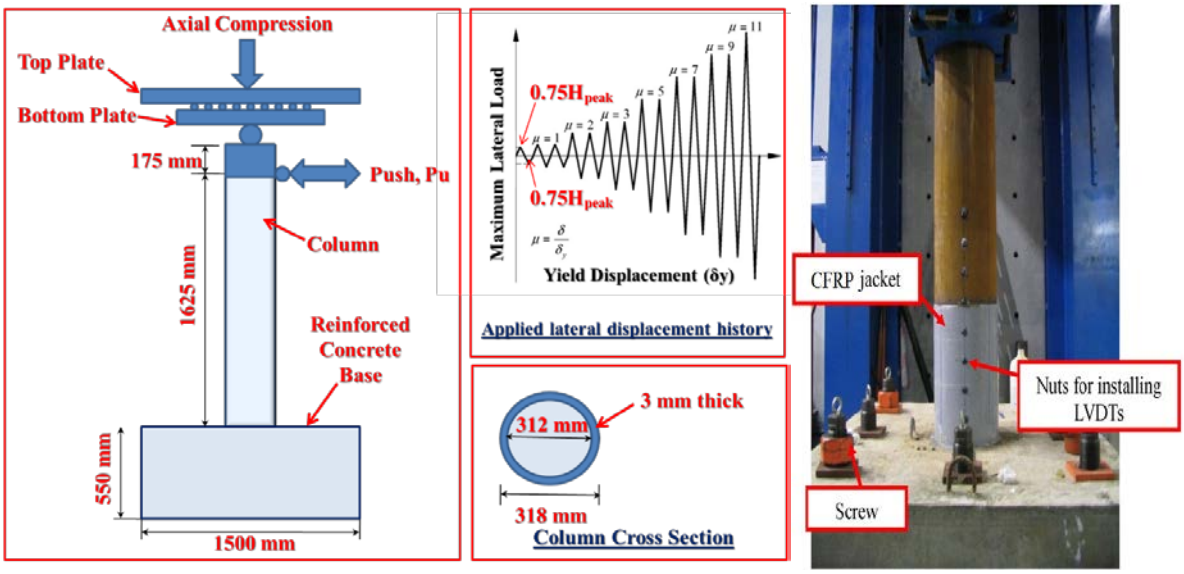

(a) **(b)** **(c)**

Figure 1. Test set-up details (dimensions are in mm) [41]: (a) Schematic diagram of test set-up, (b) Cross-section and lateral displacement history, and (c) Column wrapped with a CFRP jacket.

2.2. Description of NLFEA Program

Nonlinear finite element analysis (NLFEA) has been used in this study for its reliability and efficiency in analyzing complicated structures before being executed, saving by that costs, effort, and time. This method also detects design error, assesses the structural stresses and strains at various loads in addition to the resultant deflections, and permits the possibility of making any necessary modifications. Also, the NLFEA facilitates the ability to examine the effectiveness of a given parameter on the structure. To fulfill the purposes of this study, fourteen full-scale, strengthened-with-CFRP models were constructed and examined. The support was roller at the top of the column to allow for relative drift while kept fixed at the other end. Firstly, the column axial load was applied as the first loading step, and then the horizontal load was applied at top of the column as displacement-controlled loading to guarantee the descending part of the load-displacement behavior. In order to avoid sudden failure or on other word solution divergence as well as obtain stable analysis process, this loading was applied incrementally by providing more load sub-steps within a loading step. The steps can be divided automatically by ANSYS but the number of sub-steps must be previously inserted.

2.2.1. Description of Non-linear Finite Element Analysis (NLFEA)

The concrete material is not homogenous, brittle, and does not exhibit the same behavior in compression and tension. The SOLID 65 element has the capability to predict the concrete's response by employing a smeared crack approach in terms of ultimate uniaxial compression and tensile. In the cylinders, the compressive strength before the thermal shock was 36.6 MPa, while it was 9.8 MPa after the cylinder was thermally shocked and damaged [42]. The cylinder's tensile strength before being thermally shocked was 3.75 MPa, while it was 1.25 MPa for the damaged-by-thermal-shock ones. For this study, the Poisson's ratio was set to 0.2, and so was the shear transfer coefficient. Fig. 2(a) shows the stress-strain relationship for unconfined concrete, which describes the post-peak stress-strain behavior.

Also, the SOLID45 element has been used for its capability to interpret all directions and its efficiency in the simulation of the circular tubes of steel and the steel plates. In addition, the elastic, linear stress-strain behavior was utilized with the following settings: The Young's modulus of 203 GPa, ultimate stress of 353 MPa, the yield stress of 271 MPa, and a Poisson's ratio of 0.30. In the specimens that had been simulated, the steel was presumed to have the same fully elastic-plastic behavior in both tension and compression. The steel, used for reinforcement, had: A Poisson's ratio of 0.3, the yield stress of undamaged beams of 410 MPa, damaged beams' yield stress of 0.78 of the yielding stress, an elastic modulus of undamaged beams of 200 GPa, and 0.6 of the elastic modulus for the damaged ones [43]. Fig. 2(b) demonstrates the relationship between the stress and the strain in its ideal form. The steel plates' material was presumed linear and elastic, having a Poisson ratio of 0.3 and an elastic modulus of 200 GPa. On the other side, the CFRP material was presumably orthotropic material, having: a thickness of 0.17 mm, tensile strength of 3800 MPa, the elastic modulus of 230 GPa, and an ultimate tensile strain of 0.0169, as illustrated in Fig. 2(c).

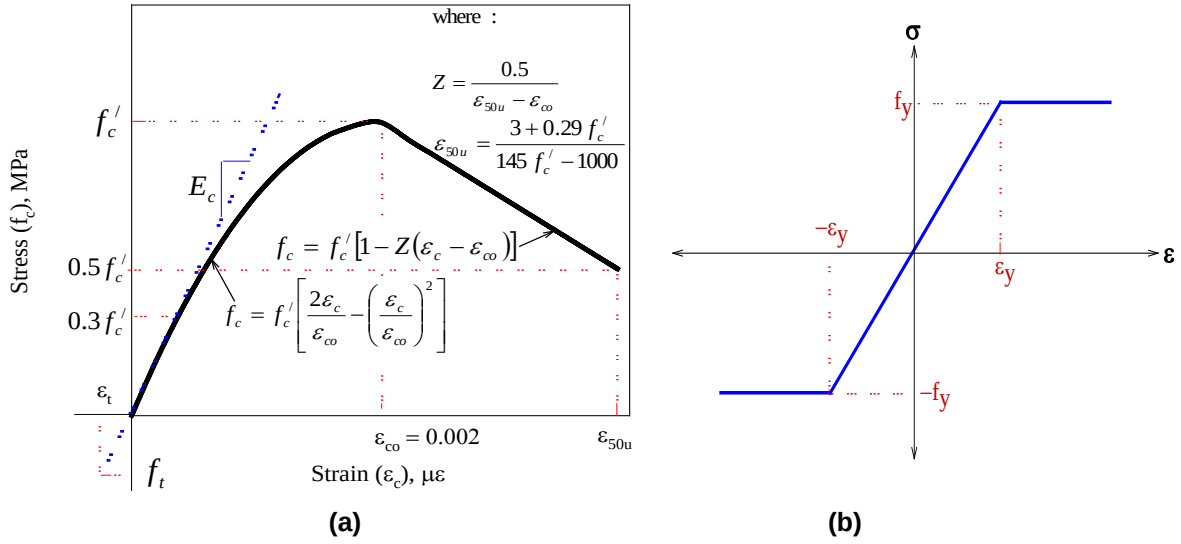

(a) **(b)**

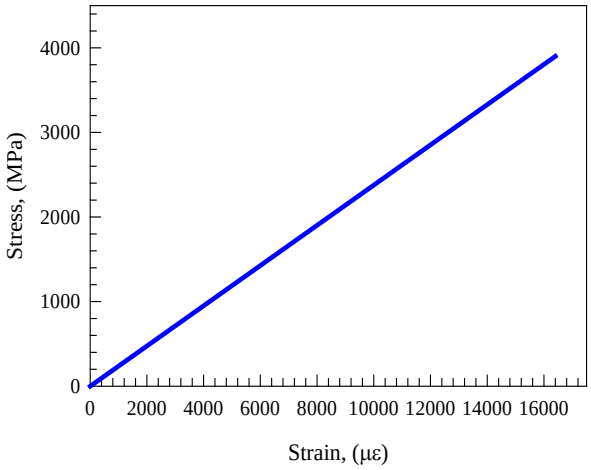

(c)

Figure 2. Stress-strain curves for: (a) unconfined concrete [42], (b) steel reinforcement [43], and CFRP composite.

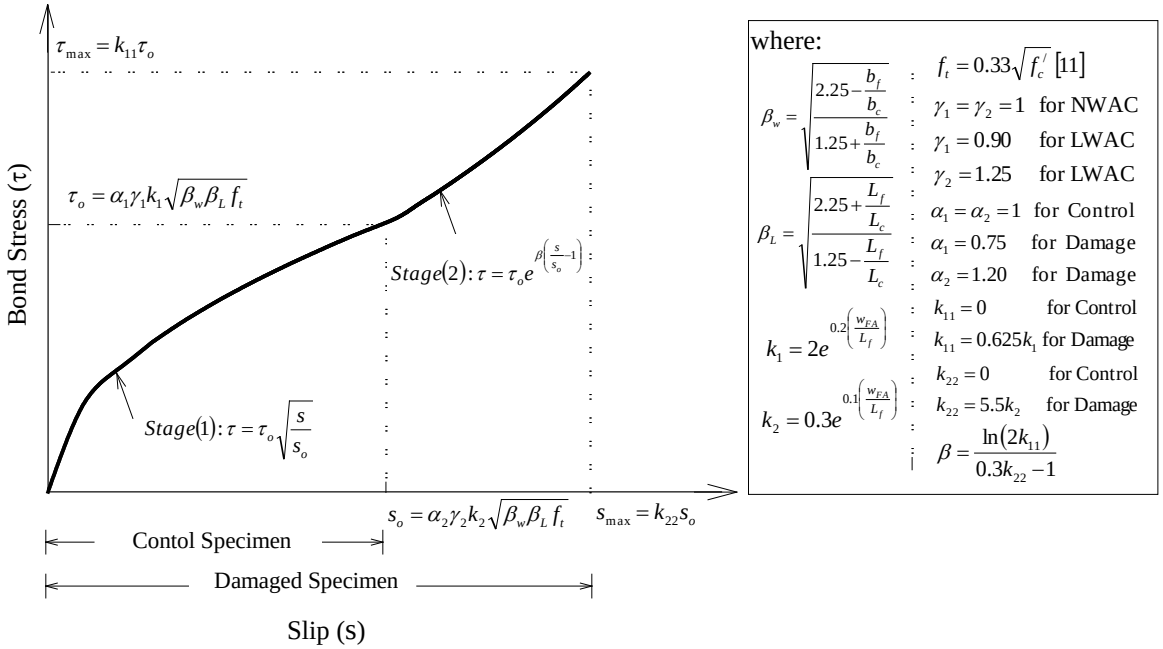

Figure 3. CFRP to concrete bond-slip model [42].

The CONTA174 element had been employed to design the zone of contact between the CFRP laminates and concrete. In this study, the utilized model of the stress-slip bonding, located between the heat-damaged concrete and the CFRP plates, had been suggested by Haddad and Al-Rousan [42], as depicted in Fig. 3. In order to investigate the performance of the RC control specimen, a simulation of a full-scale column was carried out, as illustrated in Fig. 4. Also, the density of the mesh was specified by conducting a convergence study. For more accuracy, the CFRP-concrete bonding was presumed Perfect. Fig. 4 illustrates a FEM of the meshing of the CFT specimens. The applied load had been split into a group of increments, or steps, of the load. The Newton-Raphson equilibrium iterations were employed to avail convergence at each load step's end, between the tolerance limits, with a value of 0.001 for a load increment of 0.35 kN.

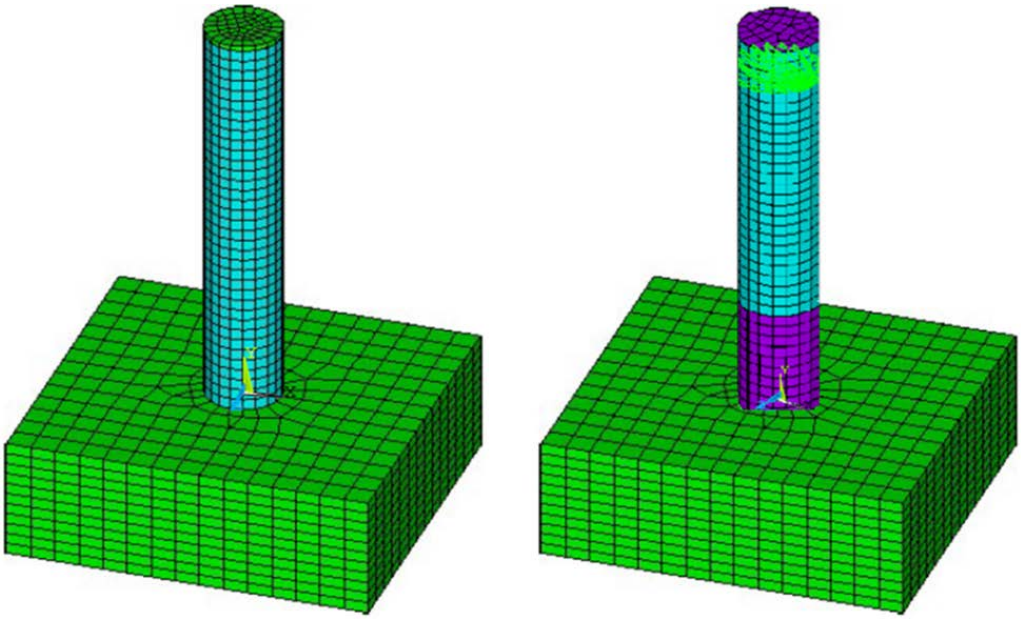

(a) (b)

Figure 4. Typical finite element meshing of the Column: (a) Without CFRP jacket and (b) With CFRP jacket.

Table 1. NLFEA configuration of confined CFT columns with CFRP composites.

Group Number	Number of CFRP layers	Column number	Un-damaged/ Damaged	CFRP strengthening configuration
1	0	CFT0-UD	Un-damaged	None
	5	CFT5-UD		five layers of CFRP
	6	CFT6-UD		six layers of CFRP
	7	CFT7-UD		seven layers of CFRP
	8	CFT8-UD		eight layers of CFRP
	9	CFT9-UD		nine layers of CFRP
	10	CFT10-UD		ten layers of CFRP
2	0	CFT0-D	Damaged	None
	5	CFT5-D		five layers of CFRP
	6	CFT6-D		six layers of CFRP
	7	CFT7-D		seven layers of CFRP
	8	CFT8-D		eight layers of CFRP
	9	CFT9-D		nine layers of CFRP
	10	CFT10-D		ten layers of CFRP

Note: C: Column, UD: un-damaged, D: Damaged

2.2.2. Investigated Parameters

In Table 1, different configurations of strengthening techniques are illustrated. All the columns were labeled as follows: CFTXX-UD/ D, where: CFT for the type of column, the XX stand for the number of CFRP layers installed, and UD/D (un-damaged/damaged). Two control CST columns were included: an un-damaged one designated as (CFT0-UD) and a damaged one labeled as (CFT0-D). The remaining specimens, 12 CFT columns, were reinforced-in-shear with sheets of CFRP, as follows: CFT5-UD and CFT5-D had five layers of CFRP (with a thickness of 0.85 mm); the CFT6-UD and CFT6-D had six layers of CFRP (thickness of 1.02 mm); the CFT7-UD and CFT7-D had seven layers of CFRP (thickness of 1.19 mm); the CFT8-UD and CFT8-D had eight layers of CFRP (thickness of 1.36 mm); CFT9-UD and CFT9-D had nine layers of CFRP (thickness of 1.53 mm), and the CFT10-UD and CFT10-D had ten layers of CFRP (thickness of 1.7 mm). The finite element modeling groups are detailed in Table 1.

2.2.3. Validation Process

By inspecting Fig. 5, a remarkable agreement has been noticed between the results of the load-drift hysteresis obtained from the NLFEA and Yu et al. [41]. A confined-by-six-CFRP-layers CFT column (labeled as LCFT-6C-106-F, according to Yu et al. [42]) was examined. Again, there was a significant agreement in

the results regarding the modes of failure and the deformed shapes (Fig. 6). The NLFEA is recommended, by many designers, to conduct additional testing and analysis to enhance the awareness of the behavior of the circular, damaged-by-thermal-shock, confined-by-CFRP CFT steel columns when undergoing simultaneous axial and lateral cyclic loading. Consequently, fourteen NLFEA models were constructed using calibrated models, aiming to assess the impact of the number of the erected CFRP layers (5 to 10 layers) and the existence of the thermal shock (with/ without).

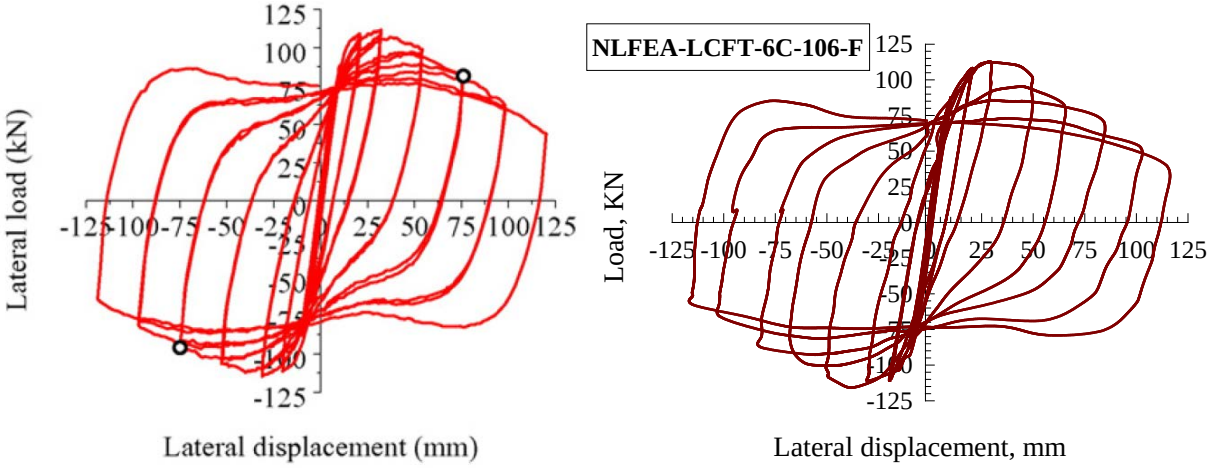

Figure 5. Validation of the FEA results: (a) Yu et al. [41] test result and (b) LCFT-6C-106-F.

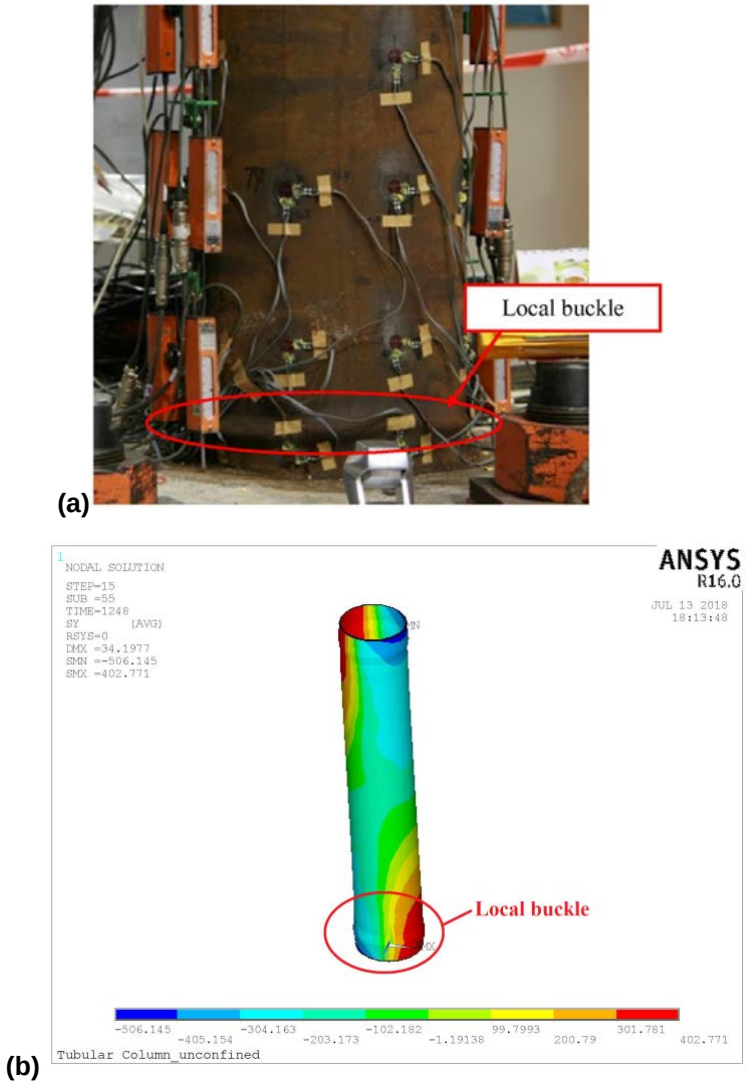

Figure 6. Deformed shapes of the FEA: (a) Yu et al. [41] test Result and (b) LCFT-6C-106-F.

3. Results and Discussion

In brief, Table 2 demonstrates the experimental results obtained from testing fourteen NLFEA models and how the study parameters have impacted them. The designation of the specimens has been explained in section 2.3. The obtained results included: the net drift, the maximum horizontal load, the strain of steel, the strain of the CFRP laminates, the degradation of stiffness, the enhancement factor of performance, and the amount of energy dissipated.

Table 2. NLFEA results of all models.

Group Number	Specimen Designation	Maximum horizontal net drift, mm	Maximum horizontal load, kN	Maximum steel strain, με	Maximum CFRP strain, με
1	CFT0-UD	102.8	102.5	1623	---
	CFT5-UD	115.8	113.9	1648	Rupture
	CFT6-UD	121.9	119.3	1674	8245
	CFT7-UD	131.7	127.8	1700	8093
	CFT8-UD	138.7	134.5	1719	7380
	CFT9-UD	144.0	138.4	1734	6786
	CFT10-UD	147.7	140.8	1745	6269
2	CFT0-D	56.6	87.1	1392	---
	CFT5-D	63.7	96.0	1432	Rupture
	CFT6-D	67.1	104.4	1460	7191
	CFT7-D	72.4	112.5	1496	6814
	CFT8-D	76.3	118.9	1526	6089
	CFT9-D	79.2	122.4	1551	5482
	CFT10-D	81.2	125.7	1560	4953

Note: yielding strain for steel is 1335 με, and CFRP ultimate strain is 8500 με.

3.1. Horizontal load-displacement hysteretic loops

Each model's stresses (of the concrete, CFRP, and steel) had been attained. Fig. 7 contours of the specimens' stresses are demonstrated for CST0-UN (control beam) and CST08-UN (un-damaged, 8 CFRP layers), showing the spots at which the stresses were condensed, particularly at the specimen's bottom end. Fig. 8 illustrates the horizontal load-displacement hysteretic loops for the un-damaged columns, while the loops of the damaged ones are depicted in Fig. 9. Both figures showed, explicitly, the influence of the layers of CFRP in improving the behavior of the CFT column and enhancing its: capacities of lateral load and net drift, in addition to the increase in the energy dissipation.

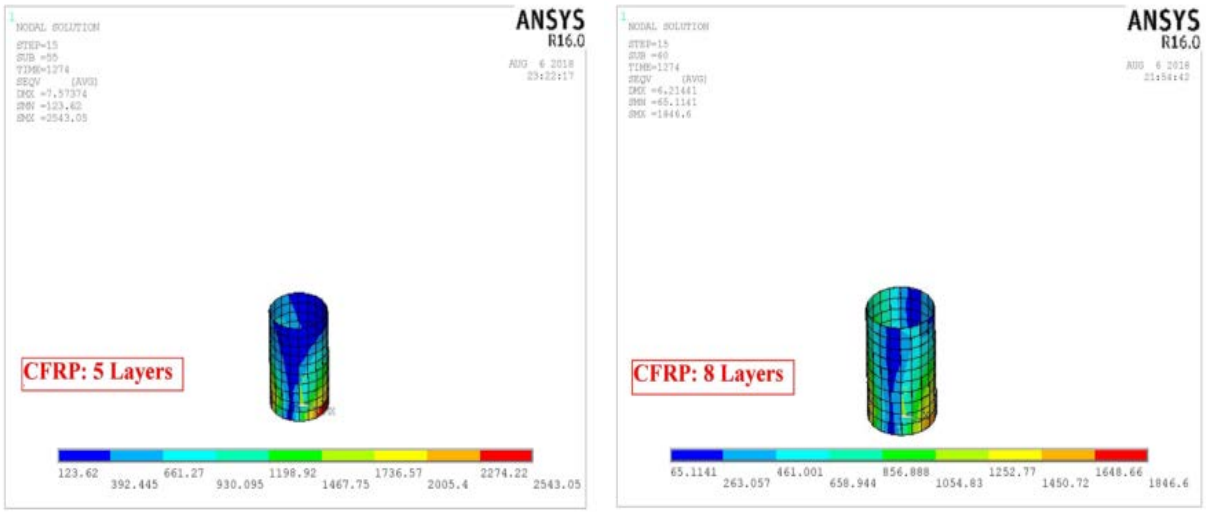

(a)

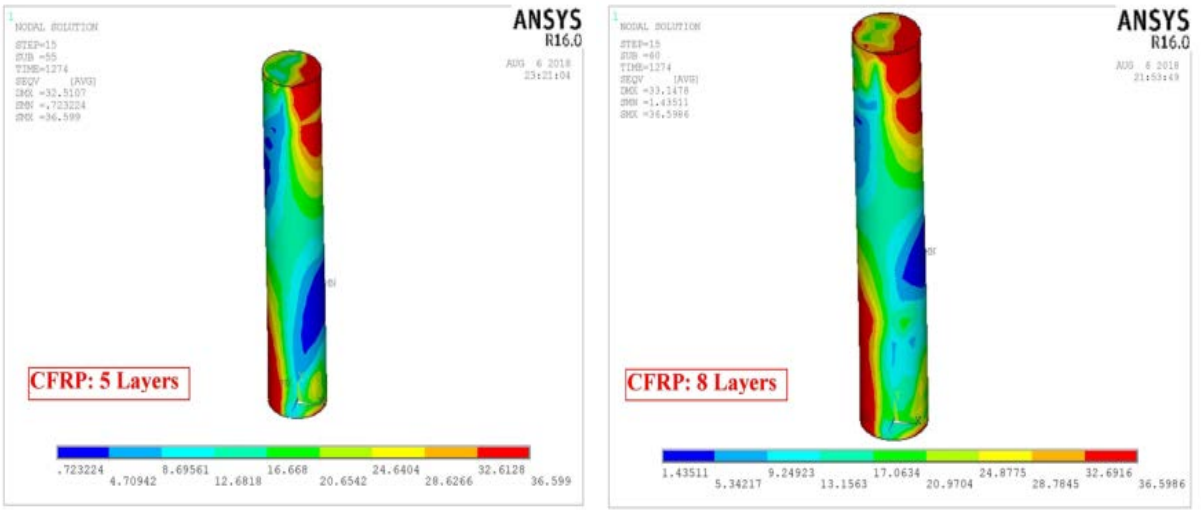

(b)

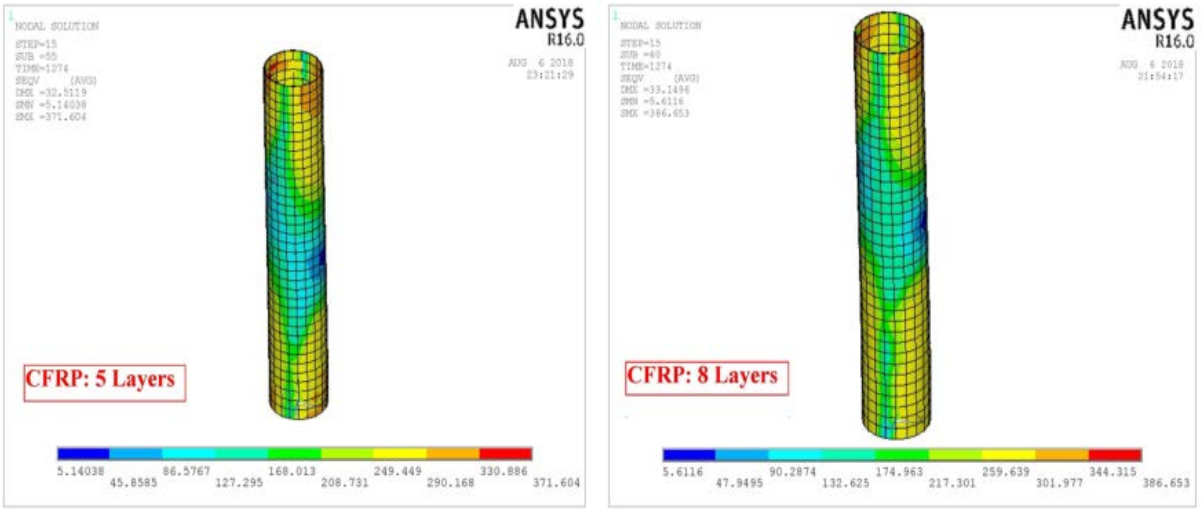

(c)

Figure 7. Sample stress contours: (a) CFRP, (b) Concrete, and (c) Steel tube.

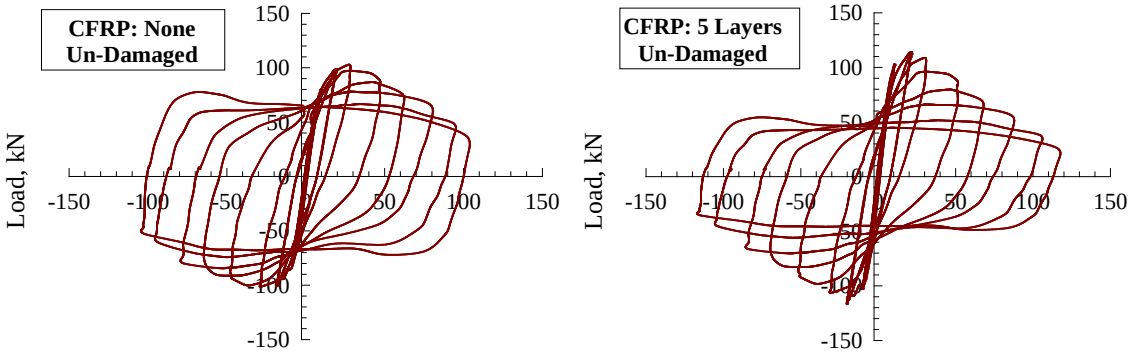

(a) **(b)**

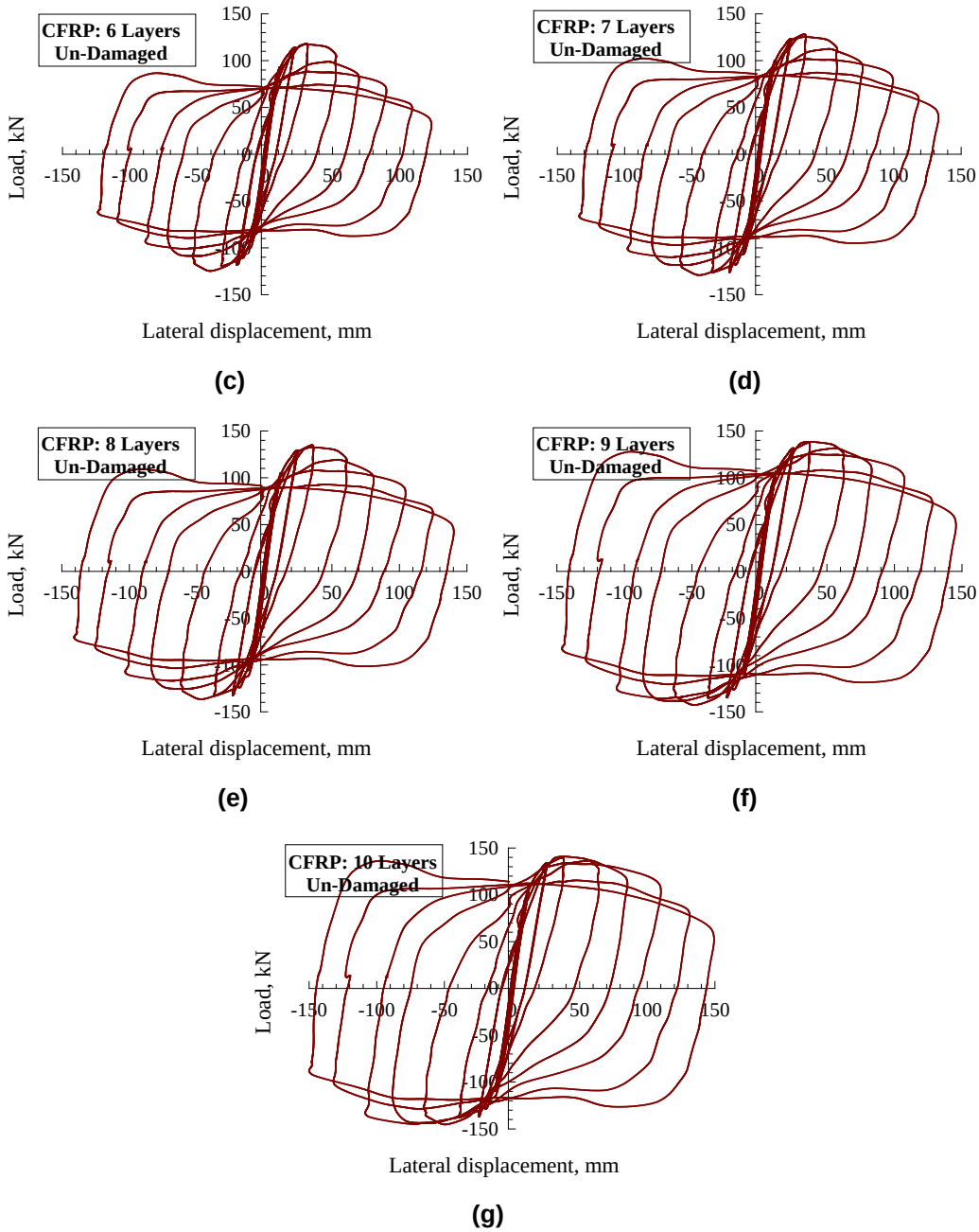

Figure 8. Horizontal load-net drift hysteresis loops for the un-damaged CFT column strengthened with (a) without CFRP, (b) 5 Layers of CFRP, (c) 6 Layers of CFRP, (d) 7 Layers of CFRP, (e) 8 Layers of CFRP, (f) 9 Layers of CFRP, and (g) 10 Layers of CFRP.

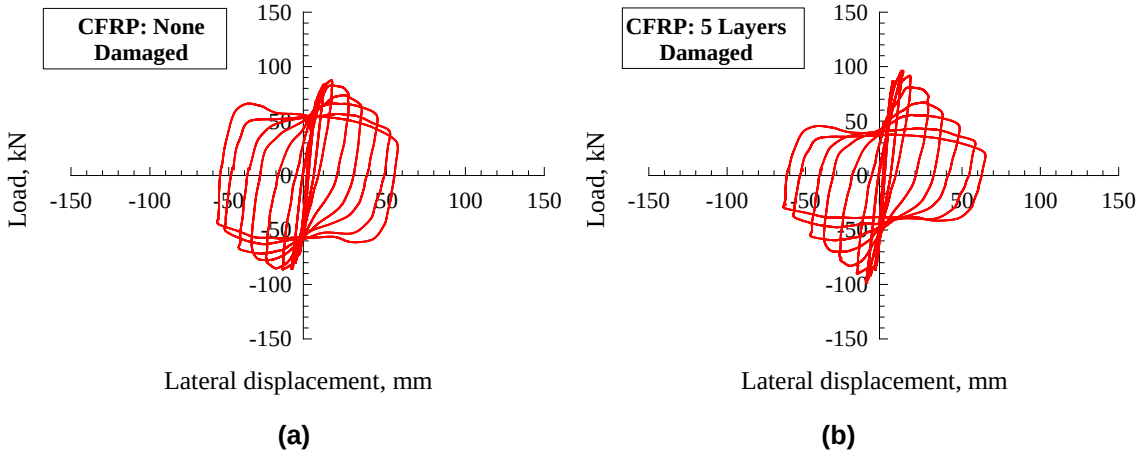

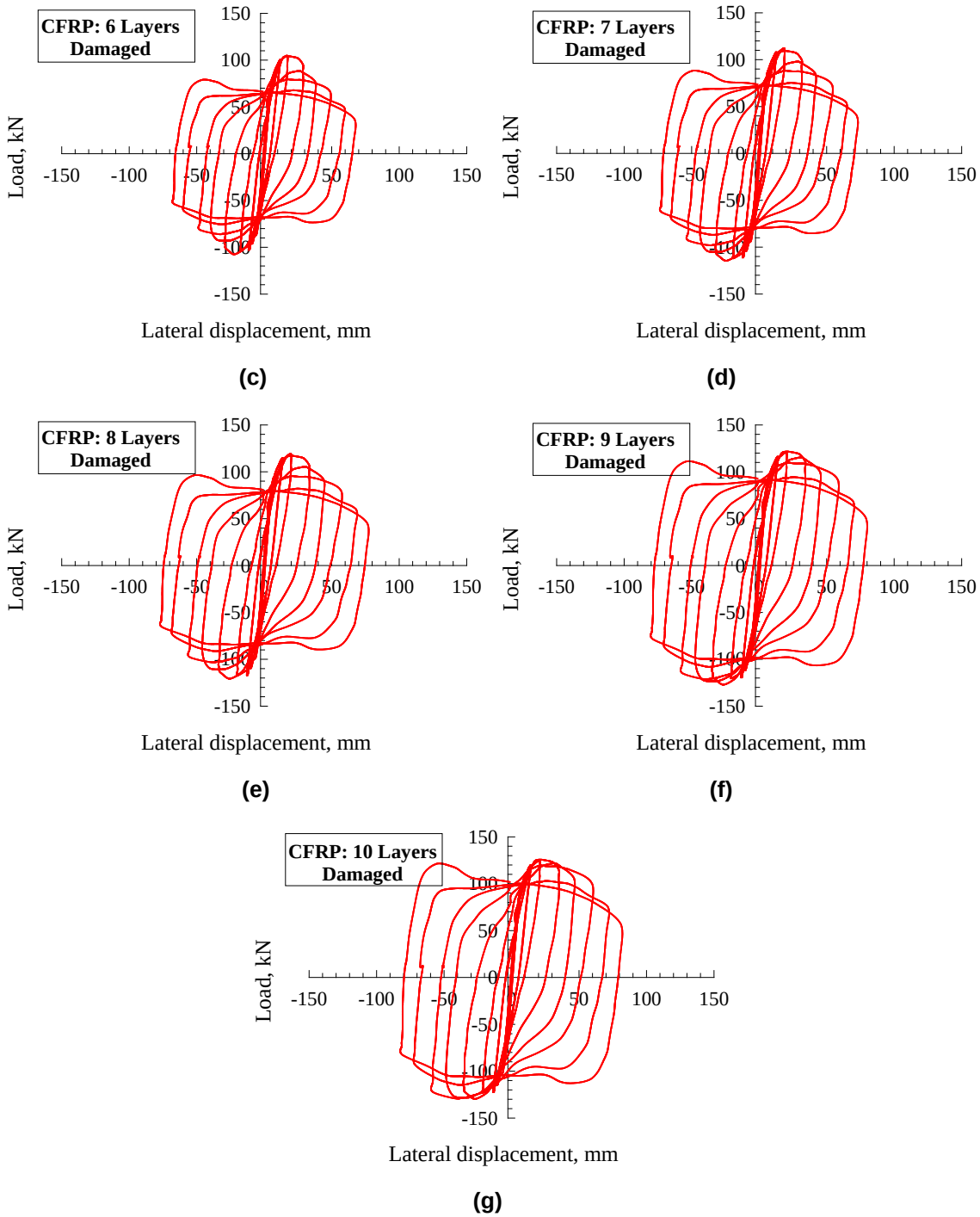

Figure 9. Horizontal load-net drift hysteresis loops for the damaged CFT column strengthened with (a) without CFRP, (b) 5 Layers of CFRP, (c) 6 Layers of CFRP, (d) 7 Layers of CFRP, (e) 8 Layers of CFRP, (f) 9 Layers of CFRP, and (g) 10 Layers of CFRP.

3.2. Lateral Load and Net Drift Capacities

Referring to Table 2 and Fig. 10 and 11, the following points have been noticed: 1) a considerable, disproportionate increase in the lateral net-drift of the un-damaged columns, while it was not as much in the lateral load capacity; 2) the number of installed CFRP layers has a considerable, positive impact on the capacities of lateral load and lateral net-drift; as installing more layers of CFRP increased both capacities, though not with the same rates; 3) the CFRP layers had no significant effect when installing less than 5 layers of them; 4) installing 8, 9, or 10 layers of CFRP had the same influence on the column behavior; 5) the maximum strain of the steel tube was slightly affected by each of the numbers of CFRP layers and the thermal shock; and, lastly, 6) the maximum strain of the CFRP reduced when the number of its layers was increased. Hence, it can be concluded that installing 5 to 8 layers of CFRP strengthened the CFT circular steel column, resulting in improving the lateral load capacity and the net drift.

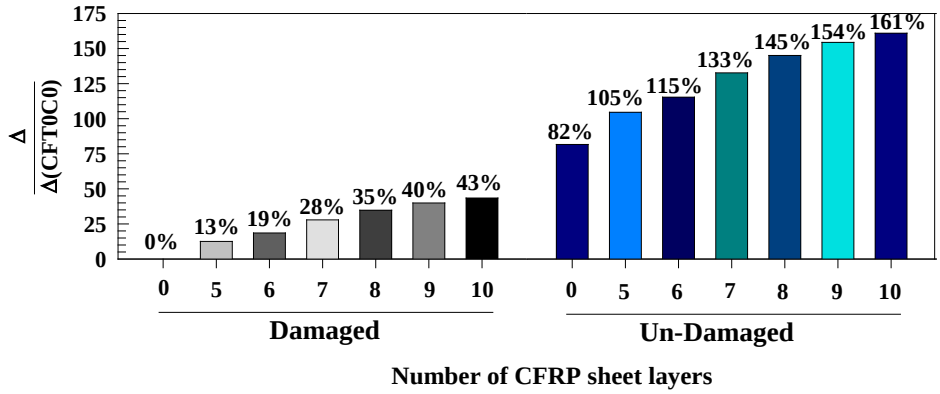

Figure 10. Effect of number of CFRP layers on the maximum horizontal net drift.

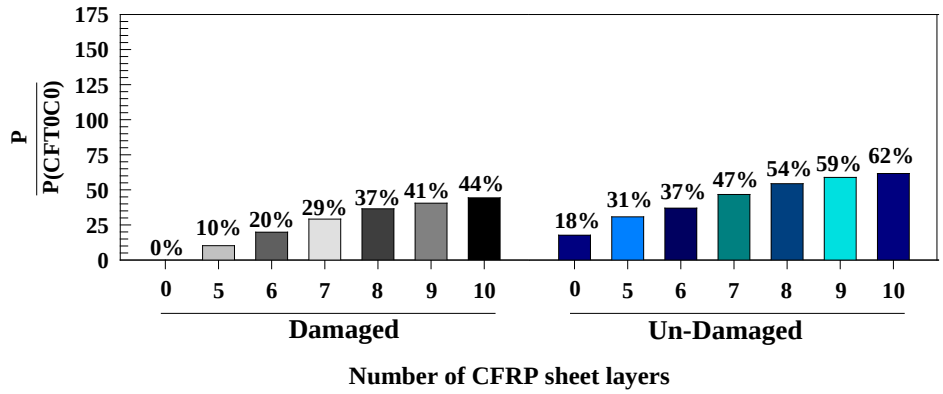

Figure 11. Effect of number of CFRP layers on the maximum horizontal load capacity.

3.3. Horizontal displacement-steel strain responses

The behavior of the CFT columns had been examined by utilizing the data of the steel tube strain. The graph of the steel tube strain vs. the emerging deflections is plotted in Fig. 12. It is worth mentioning that un-damaged CFT columns have a higher steel tube strain capacity than the damaged ones, as depicted in Table 2 and Fig. 12. To examine the influence of the study parameters on the steel strain, the steel reinforcement was modified as per the yielding value of strain, as illustrated in Fig. 13. Considering Fig. 13, it is apparent that the increase in the number of CFRP strips results in enhancing the strain of thermally-damaged steel tubes enhanced by 5 % for 0 strips, 8 % for 5 layers, 10 % for 6 layers, 12 % for 7 layers, 15 % for 8 layers, 16 % for 9 layers, and 17 % for 10 layers of CFRP. As for the un-damaged columns, the increase was: 22 % for 0 layers, 24 % for 5 layers, 26 % for 6 layers, 28 % for 7 layers, 29 % for 8 layers, 30 % for 9 layers, and 31 % for 10 CFRP layers. Also, the increase in the number of the CFRP layers from 5 to 8 layers enhanced the strain of the steel tubes proportionally. However, increasing the layers from 8 to 10 had no significant effect. So, it can be concluded that 8 layers of CFRP are the best configuration.

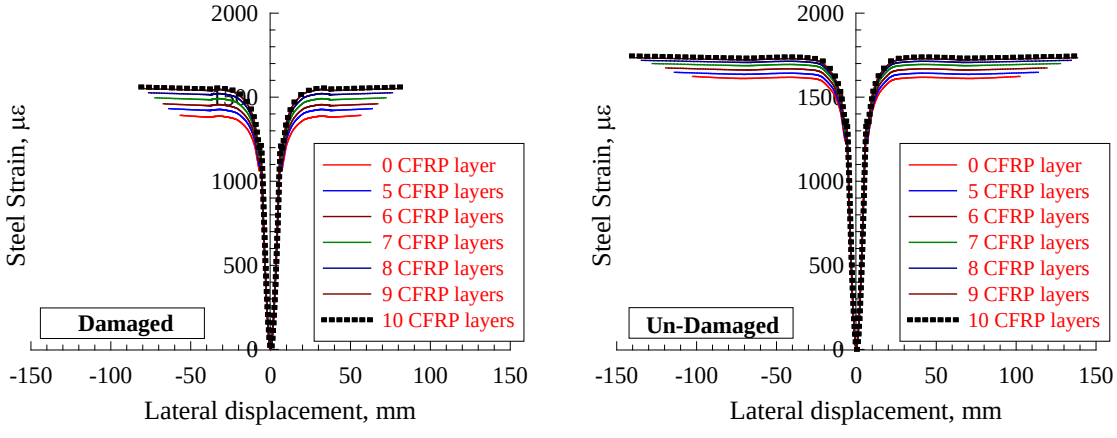

Figure 12. Steel strain CFT column: (a) Damaged and (b) Un-damaged.

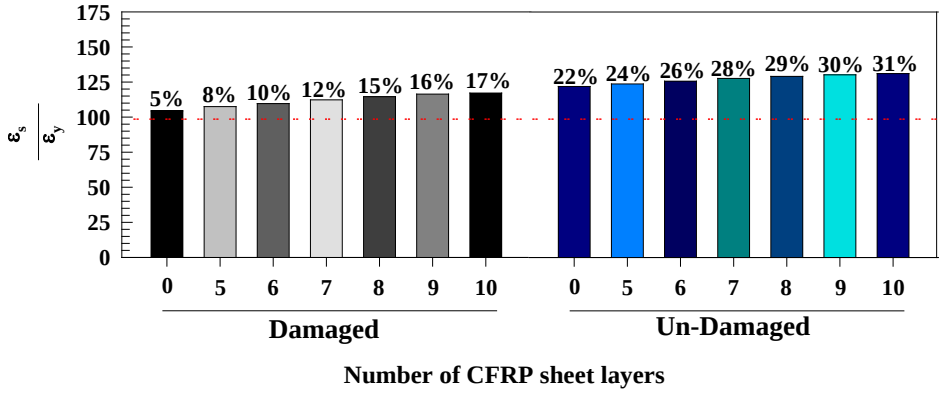

Figure 13. Effect of investigated parameters on maximum steel strain.

3.4. Horizontal displacement-CFRP strain responses

Figure 14 illustrates the graphical representation of the horizontal displacement in the reinforced-with-CFRP CST columns against the CFRP material's strain responses. The graph has two parts: 1) covers the horizontal displacements range from 0 to 10 mm, 2) is from 10 mm to failure. Fig. 14 indicates that a slight increase in the horizontal displacement results in a rapid boost in the CFRP strain. Nevertheless, a big boost in the horizontal displacement has resulted in a very slight increase in the CFRP strain. Fig. 15 also indicates that increasing the number of CFRP layers in damaged columns has resulted in a reduction in the CFRP strain, by 0 % (rupture) for 0 layers, 15 % for 5 layers, 20 % for 6 layers, 28 % for 7 layers, 64 % for 8 layers, and 42 % for 10 layers. All the percentages are of the ultimate strain value of the CFRP composite, provided by the supplier (ε_{fu}), for damaged columns. As for the un-damaged columns, the minimum reduction percentages in the CFRP strain were: 3 % for 5 layers, 5 % for 6 layers, 13 % for 7 layers, 20 % for 8 layers, and 26 % for 10 layers. Further, increasing the CFRP layers from 5 to 8 enhanced the strain of the steel tube in a proportional manner; whereas, the use of 9 or 10 layers had the same influence of 8 layers. That explicitly means that 8 layers is the best number of CFRP layers. On the other side, the thermal shock reduced the strain of CFRP material by 28 %. Finally, less than 5 layers of CFRP did not affect the strain behavior of CFRP.

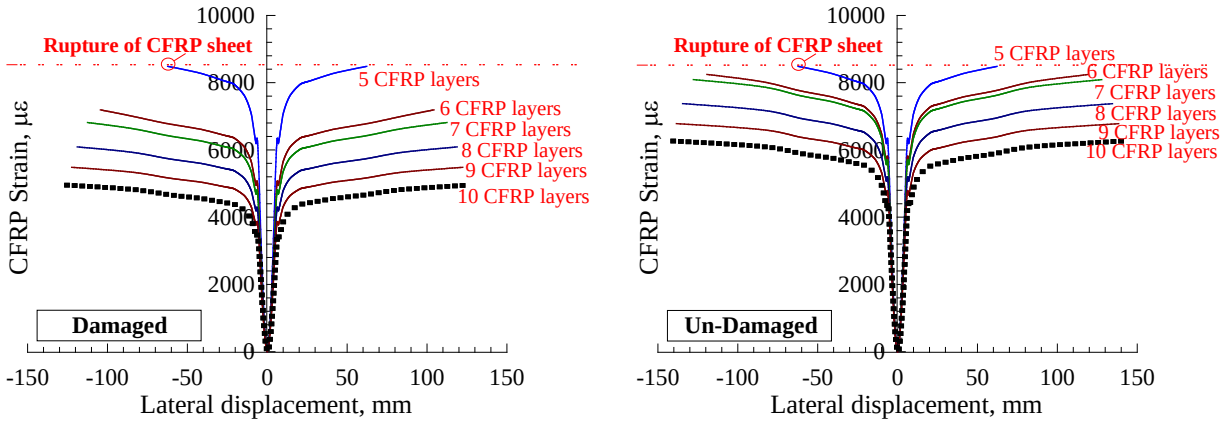

Figure 14. CFRP strain CFT column: (a) Damaged and (b) Un-damaged.

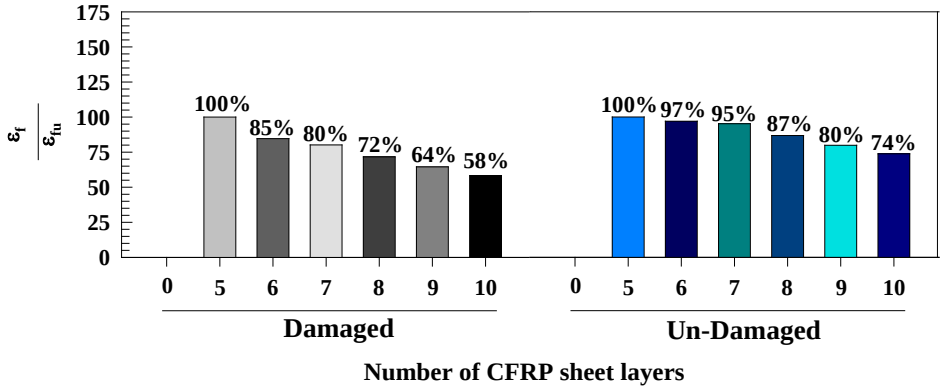

Figure 15. Effect of tested parameters on maximum CFRP strain.

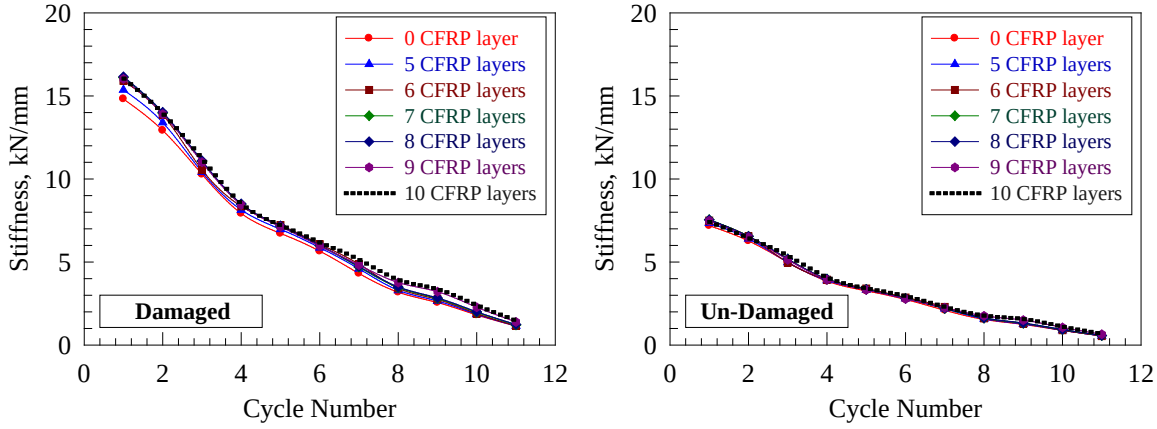

Figure 16. Stiffness degradation: (a) Damaged and (b) Un-damaged.

3.5. Stiffness degradation

In every cycle, the stiffness values were computed to determine the degradation; then, the obtained values were plotted graphically against the number of cycles of the CFT column (Fig. 16). Considering Fig. 16, the graph shows a very sharp slope for the damaged columns, where it became less and less sharp for the un-damaged ones because the intact concrete fully confined the footing-column zone. Also, neither the stiffness nor the number of cycles was significantly affected by the CFRP reinforcement technique. On the other side, the thermal shock reduced the initial stiffness, the number of cycles, while it enhanced the sharpness of stiffness degradation because of the rise of the column's compressive stress. Further, the thermal shock reduced the stiffness degradation by approximately 60 %, with respect to un-damaged columns.

3.6. Performance Enhancement Factor and Energy Dissipation

Table 3 demonstrates the increase in the lateral load capacity and net drift, referred to as load and displacement factors. They were modified in accordance to the control column CFT0-D. Every specimen's performance factor was computed by using the expression (load factor × displacement factor), to obtain a more accurate evaluation of the improvement. Compared to CFT0-D, the damaged models had a performance factor of nearly 1.25 when using 5 CFRP layers. By raising the number of the CFRP layers from 5 to 10, the performance factor increased, in a proportional manner, by almost 0.20. On the other hand, the obtained results showed no significant effect on less than 5 layers. Energy dissipation is a critical factor in seismic design. It is defined as the quantity of the energy dispersed by a structural element. It is strongly related to ductility, as they are directly proportional to each other.

As illustrated in Table 2, increasing the number of CFRP layers in un-damaged models resulted in a significant rise in the dissipated energy, where the increase was not as much in the damaged ones. It is noted that the modified energy dissipation gets along, to a limit, with the majority of the experimented cases, in terms of the performance enhancement factor. This is perfectly logical because when the performance factors have been computed, both the strength of the samples and their displacement are given the same weight. It must be stated, at this point, that it is possible to compute for the performance enhancement factor, in some cases, by assigning different ratios of weight to ductility and strength. To elaborate, when

focusing on ductility, it can be given a ratio of 0.75 % of weight, while the strength is given a ratio of 0.25 % of the weight and the other way around.

Table 3. Performance improvement factor and energy dissipation.

Group Number	Specimen Designation	Strength Factor (SF)	Displacement Factor (DF)	Performance Factor (SF*DF)	Energy dissipation, kN.mm	Normalized Energy Dissipation
1	CFT0-UD	1.82	1.18	2.14	12020	2.14
	CFT5-UD	2.05	1.31	2.68	13120	2.33
	CFT6-UD	2.15	1.37	2.95	16604	2.95
	CFT7-UD	2.33	1.47	3.41	19656	3.51
	CFT8-UD	2.45	1.54	3.78	21918	3.89
	CFT9-UD	2.54	1.59	4.04	24721	4.41
	CFT10-UD	2.61	1.62	4.22	26364	4.69
2	CFT0-D	1.00	1.00	1.00	5619	1.00
	CFT5-D	1.13	1.10	1.24	6086	1.08
	CFT6-D	1.19	1.20	1.42	7995	1.42
	CFT7-D	1.28	1.29	1.65	9511	1.69
	CFT8-D	1.35	1.37	1.84	10654	1.90
	CFT9-D	1.40	1.41	1.97	12019	2.14
	CFT10-D	1.43	1.44	2.07	12941	2.30

The models that had been reinforced with the same number of CFRP layers were subjected to a comparative study to be able to measure the impact of the axial load level on the behavior of CFT circular steel columns. The un-damaged columns had a performance enhancement factor of 2.16 with 5 CFRP layers, 2.08 with 6 layers, 2.07 with 7 layers, and 2.05 with 8 layers, 2.05 with 9 layers, and 2.04 with 10 layers. Checking these numbers shows that the value of the enhancement factor of performance, for the un-damaged columns, was around 2.0, and it was almost constant, regardless of the number of the installed CFRP layers.

3.7. Comparison of NLFEA with other results

Comparing the results obtained from NLFEA with Valipour and Foster [2], both methods showed a close resemblance of the results when subjecting concrete-filled steel (CFS) specimens to the nonlinear static and cyclic analysis. Further, the experimenting methods employed the modified fiber element technique and the total stiffness of secant to consider the material nonlinearity at section level and force interpolation concept. The impact, of each of the size and the confinement of steel tubes, on the ductility and the strength of concrete has been considered, too. Furthermore, the modeling methods had investigated the impact of local buckling, in steel tubes, on the structural strength and had the same findings.

4. Conclusions

This study presents an advanced NLFEA model for predicting seismic behavior and mode of failure of CFRP-confined CFT circular steel columns. The numerical results obtained by NLFEA model were firstly verified using experimental results obtained by Yu et al. [41]. Then, a parametric study was carried out using this NLFEA model to investigate effect of the number of CFRP layers (zero (control), five, six, seven, eight, nine and ten layers) subjected to room temperature (un-damaged) and thermal shock (damaged). The following conclusions are drawn based on the findings of this study:

1. For the modeled CFT circular steel column, the use of 5 to 10 layers of CFRP composites resulted in an increase in the lateral load and drift capacities and consequent performance factor and energy dissipation.

2. The structural lateral performance of CFT circular steel columns can be significantly enhanced through wrapping with CFRP composites.

3. The use of 9 and 10 CFRP layers did not add measurable enhancement over what was achieved with 8 CFRP layers, indicating that the optimum number of CFRP layers for the studied CFT circular steel column is 8.

4. The influence of the un-damaged column is significant and indicates a better performance than damaged columns.

5. The performance enhancement is dependent on the CFT steel column properties, thermal shock, and the number of wraps of CFRP composites, but in a non-proportional fashion. This dictates that the strengthening of any CFT circular steel column must be optimized through proper FEA modeling.

6. The findings of this study represent useful guidelines and methodology for a similar strengthening of CFT steel columns.

References

1. Han, L.H., Yang, Y.F. Cyclic performance of concrete-filled steel CHS columns under flexural loading. Journal of Construction Steel Research. 2005. 61 (4). Pp. 423–452. DOI: 10.1016/j.jcsr.2004.10.004
2. Valipour, H.R., Foster, S.J. Nonlinear static and cyclic analysis of concrete-filled steel columns. Journal of Construction Steel Research. 2010. 66 (6). Pp. 793–802. DOI: 10.1016/j.jcsr.2009.12.011
3. Mohsen, A. Issa, Rajai Z. Alrousan, Moussa A. Issa. Experimental and Parametric Study of Circular Short Columns Confined with CFRP Composites. Journal of Composite Construction. 2009. 13 (2). Pp. 135–147. DOI: 10.1061/(ASCE)1090-0268(20-09)13:2(135)
4. Al-Rousan, R.Z., Issa, M.A. Stress-strain model and design guidelines for CFRP-confined circular reinforced concrete columns. Polymer Composites. 2016. 39 (8). Pp. 2722–2733. DOI: 10.1002/pc.24262
5. Khairedin, M. Abdalla, Rajai Al-Rousan, Mohammad A. Alhassan, Nikos D. Lagaros. Finite-element modelling of concrete-filled steel tube columns wrapped with CFRP. Proceedings of the Institution of Civil Engineers: Structures and Buildings. 2020. 173 (11). Pp. 844–857. DOI: 10.1680/jstbu.19.00011
6. Mao, X.Y., Xiao, Y. Seismic behavior of confined square CFT columns. Engineering Structures. 2006. 28 (10). Pp. 1378–1386. DOI: 10.1061/(ASCE)0733-9445(2005)131:3(488)
7. Xiao, Y., He, W.H., Choi, K.K. Confined concrete-filled tubular columns. ASCE Journal of Structural Engineering. 2005. 131 (3). Pp. 488–497. DOI: 10.1061/(ASCE)0733-9445(2005)131:3(488)
8. Qin, P., Xiao, Y., Zhou, Y., Zhang, G. Research on CFRP confined circular concrete-filled steel tubular columns subjected to cyclic lateral forces. Journal of Earthquake Engineering, Engineering Vibrations. 2013. 33 (5). Pp. 190–196. DOI: 10.131-97/j.eeev.2013.05.190.qinp.024
9. Tao, Z., Han, L.H., Zhuang, J.P. Axial loading behavior of CFRP strengthened concrete-filled steel tubular stub columns. Advances in Structural Engineering. 2007. 10 (1). Pp. 37–46. DOI: 10.1260/136943307780150814
10. Park, J.W., Hong, Y.K., Choi, S.M. Behaviors of concrete filled square steel tubes con- fined by carbon fiber sheets (CFS) under compression and cyclic loads. Steel Composite Structures. 2010. 10 (2). Pp. 187–205. DOI: 10.12989/scs.2010.10.2.187
11. Abdalla, S., Abed, F., Alhamaydeh, M. Behaviour of CFSTs and CCFSTs under quasi- static axial compression. Journal of Construction Steel Research. 2013. 90 (1). Pp. 235–244. DOI: 10.1016/j.jcsr.2013.08.007
12. Wang, Z.B., Yu, Q., Tao, Z. Behaviour of CFRP externally-reinforced circular CFST members under combined tension and bending. Journal of Construction Steel Research. 2015. 106 (1). Pp. 122–137. DOI: 10.1016/j.jcsr.2014.12.007
13. Hu, Y.M., Yu, T., Teng, J.G. FRP-confined circular concrete-filled thin steel tubes under axial compression. ASCE Journal of Composites in Construction. 2011. 15 (5). Pp. 850–860. DOI: 10.1061/(ASCE)CC.1943-5614.0000217
14. Yu, T., Hu, Y.M., Teng, J.G. FRP-confined circular concrete-filled steel tubular columns under cyclic axial compression. Journal of Construction Steel Research. 2014. 94 (1). Pp. 33–48. DOI: 10.1016/j.jcsr.2013.11.003
15. Teng, J.G., Hu, Y.M., Yu, T. Stress-strain model for concrete in FRP-confined steel tubular columns. Engineering Structures. 2013. 49 (1). Pp. 156–167. DOI: 10.1016/j.engstruct.2012.11.001
16. Kodur, V., Agrawal, A. An approach for evaluating residual capacity of reinforced concrete beams exposed to fire. Engineering Structures. 2016. 110 (1). Pp. 293–306. DOI: 10.1016/j.engstruct.2015.11.047
17. Al-Ostaz, A., Irshidat, M., Tenkhoff, B., Ponnapalli, P.S. Deterioration of bond integrity between repair material and concrete due to thermal and mechanical incompatibilities. Journal of Materials in Civil Engineering. 2010. 22 (2). Pp. 136–144. DOI: 10.1061/(ASCE)0899-1561(2010) 22:2(136)
18. Nedviga, E., Beresneva, N., Gravit, M., Blagodatskaya, A. Fire Resistance of Prefabricated Monolithic Reinforced Concrete Slabs of “Marko” Technology. Adv. Intell. Syst. Comput. 2018. 692 (1). Pp. 739–749. DOI: 10.1007/978-3-319-70987-1_78
19. Hezhev, T.A., Zhurtov, A.V., Tsipinov, A.S., Klyuev, S.V. Fire resistant fibre reinforced vermiculite concrete with volcanic application. Magazine of Civil Engineering. 2018. 80 (1). Pp. 181–194. DOI: 10.18720/MCE.80.16
20. Goremikins, V., Blesak, L., Novak, J., Wald, F. Experimental investigation on SFRC behaviour under elevated temperature. Journal of Structural Fire Engineering. 2017. 8 (1). Pp. 287–299. DOI: 10.1108/JSFE-05-2017-0034
21. Goremikins, V., Blesak, L., Novak, J., Wald, F. To testing of steel fibre reinforced concrete at elevated temperature. Applications of Structural Fire Engineering. 2017. 1 (1). Pp. 48–54. DOI: 10.14311/asfe.2015.055
22. Blesak, L., Goremikins, V., Wald, F., Sajdlova, T. Constitutive model of steel fibre reinforced concrete subjected to high temperatures. Acta Polytechnica. 2016. 56 (1). Pp. 417–424. DOI: 10.14311/AP.2016.56.0417
23. Korsun, V., Vatin, N., Franchi, A., Korsun, A., Crespi, P., Mashtaler, S. The strength and strain of high-strength concrete elements with confinement and steel fiber reinforcement including the conditions of the effect of elevated temperatures. Procedia Engineering. 2015. 117 (1). Pp. 970–979. DOI: 10.1016/j.proeng.2015.08.192
24. Goremikins, V., Blesak, L., Novak, J., Wald, F. Experimental method on investigation of fibre reinforced concrete at elevated temperatures. Acta Polytechnica. 2016. 56 (1). Pp. 258–264. DOI: 10.14311/AP.2016.56.0258
25. Selyaev, V.P., Nizina, T.A., Balykov, A.S., Nizin, D.R., Balbalin, A.V. Fractal analysis of deformation curves of fiber-reinforced fine-grained concretes under compression. PNRPU Mechanics Bulletin. 2016. 1 (1). Pp. 129–146. DOI: 10.155-93/perm.mech/2016.1.09

26. Bily, P., Fladr, J., Kohoutkova, A. Finite Element Modelling of a Prestressed Concrete Containment with a Steel Liner. Proceedings of the Fifteenth International Conference on Civil, Structural and Environmental Engineering Computing. Civil-Comp Press. 2015. DOI: 10.4203/ccp.108.1
27. Bílý, P., Kohoutková, A. Sensitivity analysis of numerical model of prestressed concrete containment. Nuclear Engineering and Design. 2015. 295 (1). Pp. 204–214. DOI: 10.1016/j.nucengdes.2015.09.027
28. Al-Rousan, R. Behavior of two-way slabs subjected to drop-weight. Magazine of Civil Engineering. 2019. 90(6). Pp. 62–71. DOI: 10.18720/MCE.90.6
29. Al-Rousan, R. The impact of cable spacing on the behavior of cable-stayed bridges. Magazine of Civil Engineering. 2019. 91 (7). Pp. 49–59. DOI: 10.18720/MCE.91.5
30. Krishan, A., Rimshin, V., Erofeev, V., Kurbatov, V., Markov, S. The energy integrity resistance to the destruction of the long-term strength concrete. Procedia Engineering. 2015. 117 (1). Pp. 211–217. DOI: 10.1016/j.proeng.2015.08.143
31. Korsun, V., Vatin, N., Korsun, A., Nemova, D. Physical-mechanical properties of the modified fine-grained concrete subjected to thermal effects up to 200°S. Applied Mechanics and Materials. 2014. 633–634. Pp. 1013–1017. DOI: 10.4028/www.scientific.net/AMM.633-634.1013
32. Korsun, V., Korsun, A., Volkov, A. Characteristics of mechanical and rheological properties of concrete under heating conditions up to 200°C. MATEC Web Conference. 2013. 6 (1). Pp. 07002. DOI: 10.1051/matecconf/20130607002
33. Petkova, D., Donchev, T., Wen, J. Experimental study of the performance of CFRP strengthened small scale beams after heating to high temperatures. Construction and Building Materials. 2014. 68 (1). Pp. 55–61. DOI: 10.1016/j.conbuildmat.20-14.06.014
34. Ji, G., Li, G., Alaywan, W. A new fire resistant FRP for externally bonded concrete repair. Construction and Building Materials. 2013. 42 (1). Pp. 87–96. DOI: 10.1016/j.conbuildmat.2013.01.008
35. Trentin, C., Casas, J.R. Safety factors for CFRP strengthening in bending of reinforced concrete bridges. Composite Structures. 2015. 128 (1). Pp. 188–198. DOI: 10.1016/j.compstruct.2015.03.048
36. Ferrari, V.J., Hanai, J.B. de, Souza, R.A. de. Flexural strengthening of reinforcement concrete beams using high performance fiber reinforcement cement-based composite (HPFRCC) and carbon fiber reinforced polymers (CFRP). Construction and Building Materials. 2013. 48 (1). Pp. 485–498. DOI: 10.1016/j.conbuildmat.2013.07.026
37. Attari, N., Amziane, S., Chemrouk, M. Flexural strengthening of concrete beams using CFRP, GFRP and hybrid FRP sheets. Construction and Building Materials. 2012. 37 (1). Pp. 746–757. DOI: 10.1016/j.conbuildmat.2012.07.052
38. Kara, I.F., Ashour, A.F., Körog˘lu, M.A. Flexural behavior of hybrid FRP/steel reinforced concrete beams. Composite Structures. 2015. 129 (1). Pp. 111–121. DOI: 10.1016/j.compstruct.2015.03.073
39. Rajai, Z., Al-Rousan, I., Abo-Msamh. Bending and torsion behaviour of CFRP strengthened RC beams. Magazine of Civil Engineering. 2019. 92 (8). Pp. 48–62. DOI: 10.18720/MCE.92.4
40. Rajai, Z., Al-Rousan. The shear behavior of CFRP strengthened RC beams. Magazine of Civil Engineering. 2020. 98 (6). Art. No. 9810. DOI: 10.18720/MCE.98.10
41. Yu, T., Hu, Y.M., Teng, J.G. Cyclic lateral response of FRP-confined circular concrete-filled steel tubular columns. Journal of Constructional Steel Research. 2016. 124 (1). Pp. 12–22. DOI: 10.1016/j.jcsr.2016.05.006
42. Rajai, Z., Al-Rousan, I. Behavior of CFRP strengthened columns damaged by thermal shock. Magazine of Civil Engineering. 2020. 97 (5). Art. No. 9708. DOI: 10.18720/MCE.99.10
43. Rajai, Z., Al-Rousan. Behavior of strengthened concrete beams damaged by thermal shock. Magazine of Civil Engineering. 2020. 94 (2). Pp. 93–107. DOI: 10.18720/MCE.94.8

Contacts:

Rajai Al-Rousan, rzalrousan@just.edu.jo